Three-Dimensional Continuum Simulation of Biological Ion Channels

T.A. van der Straaten*, J. Tang*, R.S. Eisenberg*, U. Ravaioli** and N. Aluru**
*Dept of Molecular Biophysics and Physiology, Rush Medical College
1750 W Harrison St, Chicago, IL 60612, trudyv@uiuc.edu, jtang@rush.edu, beisenbe@rush.edu
** Beckman Institute for Advanced Science and Technology, University of Illinois at Urbana-Champaign
405 N Mathews Ave, Urbana, IL 61801, ravaioli@uiuc.edu, aluru@uiuc.edu

ABSTRACT

We present a self-consistent continuum 3-D simulation of ion permeation through the *ompF* porin channel, a protein found in the membrane of the *e-coli* bacterium. The model is based on the simultaneous solution of Poisson's equation, which captures Coulomb interactions and a continuity equation for each ion species, describing permeation down an electrochemical gradient. Water is treated as a uniform background medium with a specific dielectric constant and macroscopic current flow is resolved by assigning an appropriate mobility/diffusivity to each ionic species. Using this model with a single diffusivity for each ion species we predict the current-voltage relations for *ompF* porin for a wide range of experimental conditions. Agreement with experimental measurements is remarkably good given that the model uses the same two adjustable parameters (diffusivity for each ion species) for the entire set of experimental conditions.

Keywords: Ion channels, Poisson-Nernst-Planck, Transport simulation, *ompF* Porin, Nanotechnology.

1 INTRODUCTION

Found in every form of life, ion channels are proteins that form nanoscopic aqueous tunnels in the otherwise almost impermeable membranes of biological cells. Each channel is made of a chain of amino acids carrying a strong spatially varying electric charge. By regulating the passive transport of ions across the cell membrane, ion channels maintain the correct internal ion composition that is crucial to cell survival and function. Ion channels directly control electrical signaling in the nervous system, muscle contraction, and the delivery of many clinical drugs [1]. Most channels have the ability to selectively transmit or block a particular ion species and many exhibit gating properties similar to electronic devices. Understanding the structure and role of ion channels in cell function is therefore central to understanding cell behavior as a whole. The possibility of incorporating ion channels in the design of novel bio-devices also presents exciting opportunities and great challenges.

Molecular dynamics simulations [2], which resolve channel physics at the atomic level, are presently limited to simulation times of not more than a few nanoseconds, due to the small timesteps (~ femtoseconds) required to resolve individual ion trajectories and large ensemble sizes needed to adequately represent ion concentrations. However, reliable estimates of steady-state channel currents require hundreds of simulations for durations of the order of milliseconds, thus preventing a direct experimental validation of the simulation [3]. Additional problems associated with external boundary conditions, biased trajectory sampling and image force effects at dielectric discontinuities also make molecular dynamics simulations difficult to implement. An alternative approach based on a mean-field electrodiffusion model, in which the ion-water interactions are described by macroscopic transport parameters, does not suffer these difficulties and has been found to describe ion permeation through ion channels surprisingly well [4].

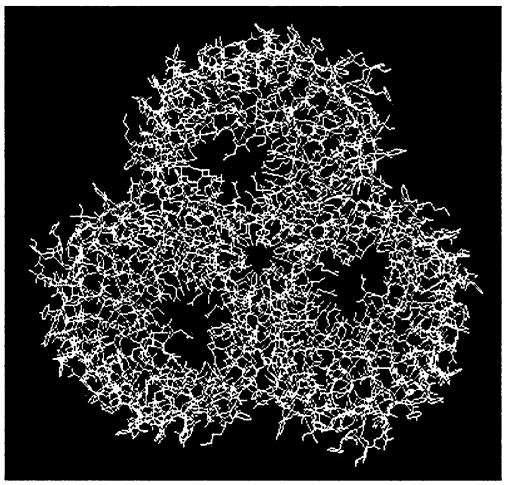

Figure 1: Molecular structure of *ompF* porin [5].

In this paper we present a self-consistent 3-D continuum model of ion (K^+ and Cl^-) permeation through the *ompF* porin channel, a trimeric protein that resides in the outer membrane of the *e-coli* bacterium. The structure of *ompF* porin is both well-known [5] and extremely stable in a wide variety of salt concentrations. Figure 1 shows clearly the three separate monomer channels that link together to form the porin trimer. Each monomer appears to operate independently making porin an interesting candidate for multilevel logic devices. In the next section we outline the details of our model and its application to the

porin channel. In section 3 we present the results obtained with this model. In particular, the current-voltage characteristics predicted by the simulation are compared with experimentally measured curves. Section 4 concludes with a discussion of this work and future plans.

2 POISSON-DRIFT-DIFFUSION MODEL

The channel system studied here is comprised of a porin trimer *in situ* in a cell membrane, immersed in an aqueous bath of *KCl*. The channel thus provides a pathway for K^+ and Cl^- ions to cross the otherwise impervious membrane. Experimentally it is possible to maintain different salt concentrations on either side of the membrane (hereafter referred to as C_{left} and C_{right}). Electrodes can also be immersed in the baths to apply a fixed bias across the channel/membrane system.

The electrostatic environment of the porin channel is determined by (i) mobile ions continuously permeating through the open channel, (ii) fixed (permanent) charges that reside on the protein itself, and (iii) the charges in the aqueous baths and on the electrodes immersed therein. The latter maintain the boundary conditions of the system of constant concentration and transmembrane potential. Since the ion flux depends on the local field, which in turn depends on all the charges in the system, both mobile and fixed, it is clear that a correct model of ion transport must include the local electric field in a self-consistent manner. Accordingly, the local electric potential φ is described by Poisson's Equation,

$$\nabla\bullet(\varepsilon\nabla\varphi) = -(\rho_{fixed} + \rho_+ + \rho_-) \tag{1}$$

where ε is the dielectric constant, and ρ_{fixed}, ρ_+ and ρ_- are the charge densities per unit volume of fixed charges residing on the protein, K^+ ions and Cl^- ions, respectively. Current flow $j_\pm$ is described by the drift-diffusion equation

$$j_\pm = -(\mu_\pm \rho_\pm \nabla\varphi \pm D_\pm \nabla\rho_\pm) \tag{2}$$

where $\mu_\pm$ and $D_\pm$ are, respectively, the mobilities and diffusivities of the ionic species. Conservation of charge dictates

$$\nabla\bullet j_\pm + \frac{\partial\rho_\pm}{\partial t} = S_\pm \tag{3}$$

where $S_\pm$ can be any form describing the details of ion binding and other chemical phenomena that populate or deplete the ion densities. In the present model we do not consider such phenomena and set $S_\pm = 0$. We seek a steady-state solution for φ, ρ_+ and ρ_- that simultaneously satisfies equations (1)-(3) subject to specific Dirichlet boundary conditions at the electrodes (C_{left}, C_{right} and V_{bias}).

The model described above was implemented using the PROPHET simulator [6], a rapid prototyping computational platform originally developed by C. Rafferty (Lucent) and currently being extended by Prof. Dutton's group at Stanford University. The PROPHET simulator uses the "dial-an-operator" methodology to construct systems of partial differential equations by combining existing differential operators described using a relatively simple scripting syntax. Equations (1) – (3) and the boundary conditions are readily constructed using existing PROPHET operators. Physical properties (e.g., dielectric constant, diffusivities) are assigned to the different regions of the domain at run-time. For the results presented here we use ε = 80, 20 and 2, for the aqueous, protein and membrane regions, respectively.

3 RESULTS

In this section we show current-voltage (*I-V*) curves for ion permeation through the open porin trimer, comparing simulation with experiment [7]. Experimental data are indicated by the thick line. The discontinuities evident in some of the experimental data indicate that the channel has closed spontaneously over that particular range of applied voltages. For each set of experimental conditions we show two sets of simulation results obtained with:

(I) $D_+ = D_- = 8.0\times10^{-6}\,cm^2 s^{-1}$ (solid line, circles)

(II) $D_+ = D_- = 1.02\times10^{-5}\,cm^2 s^{-1}$ (dashed line, squares)

Mobilities were assigned using the Einstein relations. The diffusivity used in (I) was chosen to give the best fit to the *I-V* measurements in 100mM *KCl* symmetric ($C_{left} = C_{right}$) bath concentrations. However, as the bath concentrations are increased and made asymmetric the agreement with experiment was found to decrease. Accordingly, we increased the diffusivity in proportion to the average ratio of the experimental to simulation conductance (near zero current) and performed a second simulation (II), which gave improved fits to experiment at higher bath concentrations.

3.1 Symmetric Bath Concentrations

Figure 3 shows both the experimentally measured and computed *I-V* curves obtained in symmetric solutions of (a) 100mM, (b) 250mM and (c) 500mM *KCl*. The asymmetry in both the experimental and computed curves, at low (100mM) and intermediate (250mM) concentrations reflects the asymmetry inherent in the porin structure and the distribution of fixed charges. As the bath solution is increased the degree of asymmetry decreases. The simulations performed with the lower diffusivity (I) fit the experiment better at 100mM and 500mM bath concentrations while the higher diffusivity (II) gives a slightly better fit at 250mM.

Computational Nanoscience 2001, (www.cr.org), ISBN 0-9708275-3-9.

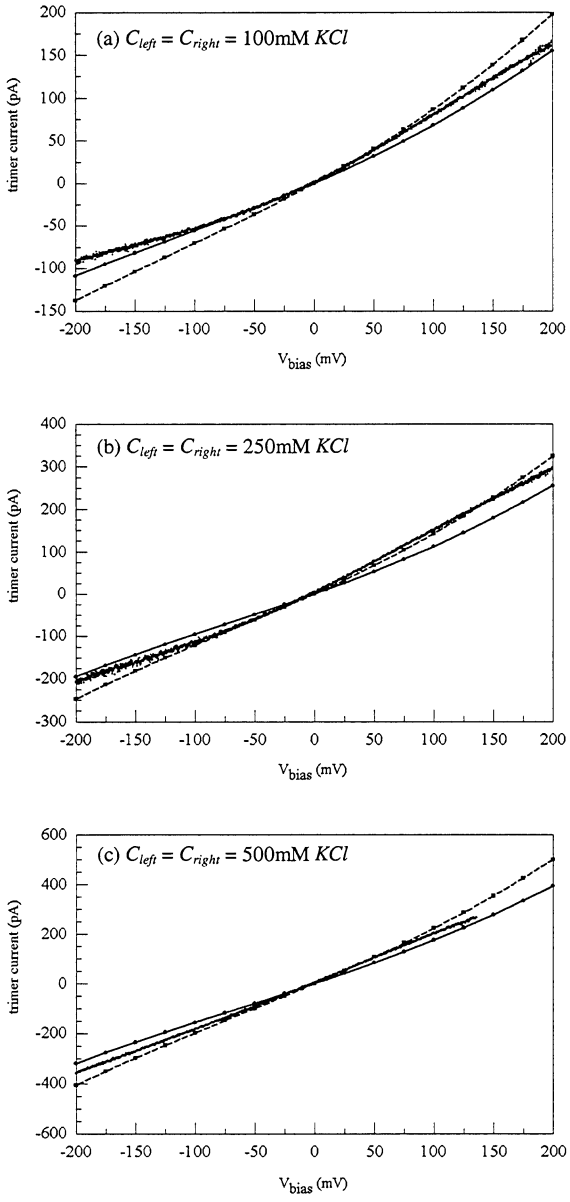

Figure 3: Comparison of drift-diffusion model with experimental *IV* curves in symmetric bath concentrations, (a) 100mM (b) 250mM, and (c) 500mM.

3.2 Asymmetric Bath Concentrations

Figures 4 (a)-(d) compare the simulation with experimental *IV* curves in asymmetric concentrations of *KCl*. For the case C_{left} = 100mM, C_{right} = 250mM (Figure 4 (a)) the lower value of diffusivity fits the experiment better at negative applied bias while the higher diffusivity fits better at positive bias. When the bath concentrations are swapped however, as in Figure 4 (b), a higher diffusivity gives a better fit over most of the range of data.

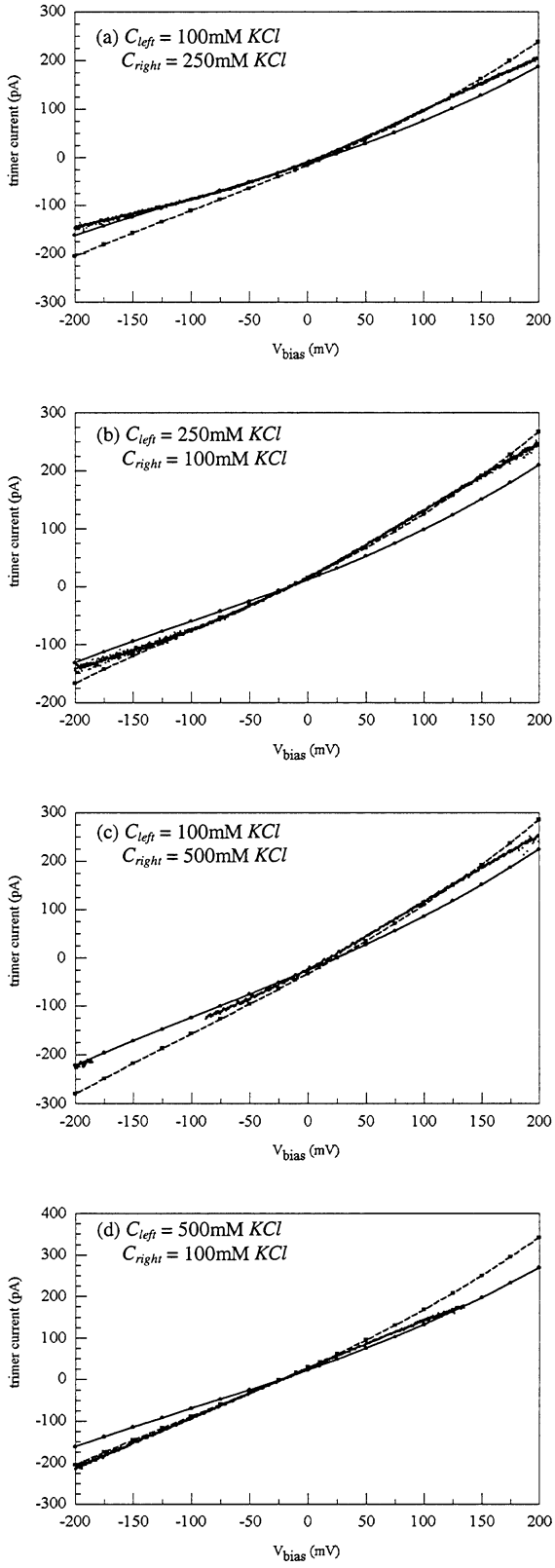

Figure 4: Comparison of drift-diffusion model with experimental *IV* curves in asymmetric bath concentrations

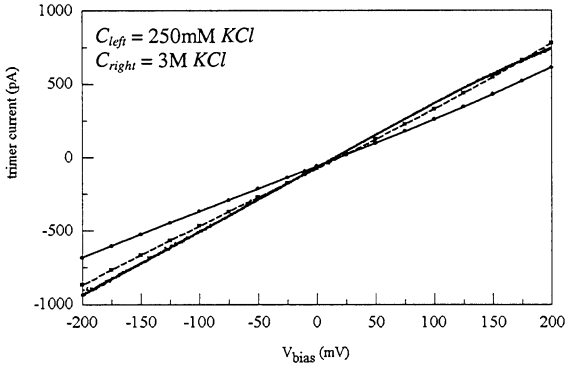

Figure 5: Comparison of drift-diffusion model with experiment for C_{left} = 250mM, C_{right} = 3M.

This dependence of the effective diffusivity on the alignment of the porin channel with respect to the baths is more apparent in Figures 4 (c) C_{left} = 100mM, C_{right} = 500mM and (d) C_{left} = 500mM, C_{right} = 100mM. Figure 5 shows a more extreme asymmetric bath concentration with C_{left} = 250mM, C_{right} = 3M.

3.3 Distribution of Charge and Potential

Figures 6 shows (a) K^+ ion density and (b) Cl^- ion density, on a 2-D slice through the 3-D computational domain, with $C_{left} = C_{right}$ = 100mM *KCl*, V_{bias} = 200 mV, and $D_+ = D_- = 8.0\times10^{-6} cm^2 s^{-1}$. The slice intersects only one of the three monomer channels. Ions accumulate in regions of strong fixed charge residing on the amino acids.

4 DISCUSSION

The success of the Poisson-drift-diffusion theory in fitting experimentally determined *IV* curves is remarkably good given the fact that we have used only two adjustable parameters (diffusivity of each ionic species) to simulate a variety of bath concentrations over a large range of voltages applied across the membrane. Clearly, some values of diffusivity give a better fit with experimental data over particular range of concentrations and bias voltages. Indeed a single uniform diffusivity cannot capture all the physical effects affecting ion transport in an inherently three-dimensional restricted volume. The next logical step is therefore to incorporate a functional form for the diffusivity of each ionic species that includes a dependence on position (or local field) and/or ion density.

ACKNOWLEDGEMENTS

This work was partially supported by the NSF Distributed Center for Advanced Electronics Simulation (DesCArtES) grant ECS 98-02730, DARPA contract N65236-98-1-5409 (B.E.) and an NSF KDI grant to the University of Illinois. The authors thank E. Jakobsson and the staff of the Computational Biology group at the University of Illinois for useful discussions, and R.W. Dutton, Z. Yu and D. Yergeau of Stanford University for assistance with implementation of PROPHET applications.

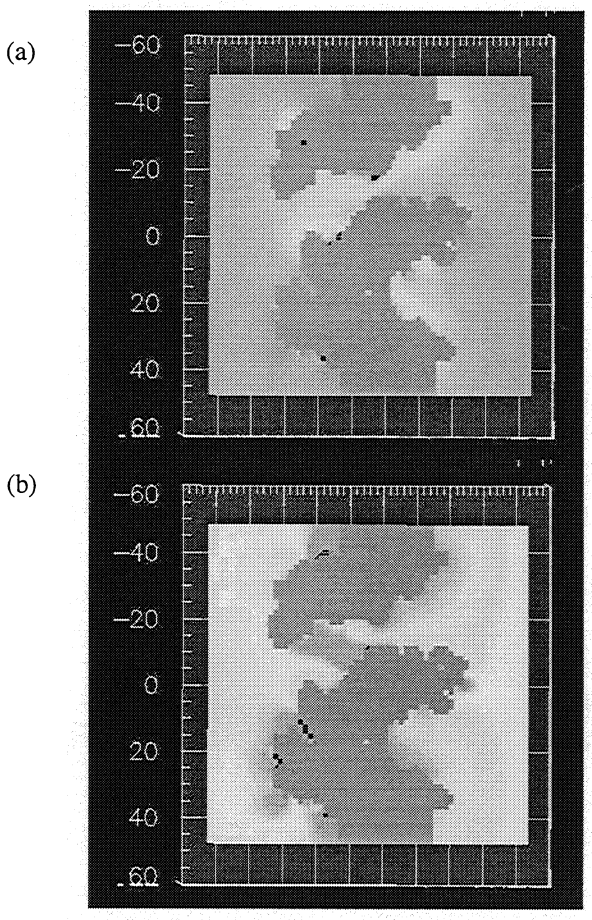

Figure 6: (a) K^+ ion density and (b) Cl^+ ion density, on a 2-D slice through the 3-D computational domain.

REFERENCES

[1] Eisenberg B. 1998. Ionic Channels in Biological Membranes – electrostatic analysis of a natural nanotube. *Contemp. Phys* 39: 447-466.

[2] Roux, B. and M. Karplus. 1994. Molecular Dynamics Simulations of the Gramicidin Channel. *Annu. Rev. Biophys. Biomol. Struct.* 23:731-761

[3] Nonner, W., D.P. Chen and R.S. Eisenberg.1999. Progress and Prospects in Permeation. *J. Gen. Physiol.* 113:773-782

[4] Chen, D.P., A. Tripathy, G. Meissner and R.S. Eisenberg. 1997. Permeation Thorught the Calcium Release Channel of the Cardiac Muscle. *Biophys. J.* 73:1337-1354.

[5] Cowan, S.W., T. Schirmer, G. Rummel, M. Steiert, R. Ghosh, R.A. Pauptit, J.N. Jansonius and J.P. Rosenbusch. 1992. *Nature*. 358:727-733.

[6] For information on PROPHET go to the website http://www-tcad.stanford.edu/.

[7] Tang, J.M. and R.S. Eisenberg, Private communication.